

QSPECTパッケージ内でDTARG法が組み込まれており、SPECT装置に依存しない脳血流の定量画像が得られる。

5) QSPECTパッケージによる SPECT品質管理

SPECTデータの標準化を行うためには、定期的にSPECT装置の品質管理をすることが重要である。QSPECTパッケージでは、品質管理のために前節で述べたCCFを計算するプログラムを組み込んでいる。さらに、BCF (Becquerel calibration factor) と呼ばれるSPECT装置間、あるいはコリメータ間の感度の違いを補正する係数を管理可能である。Fig. 2にQSPECTパッケージ内のディレクトリ構造を示すが、この図に見られるように各装置、各コリメータ、各核種で、BCF, CCF, TDCSパラメータを管理しており、この構造を利用することにより、多くのSPECT装置に対応が可能となっている。

さらに、各施設、各SPECTカメラで得られたBCF, CCFを集計したデータベースは、施設間の評価をする上で重要なデータとなり、今まで不可能とされてきたSPECTによる大規模多施設評価研究の道を拓くものである。

5. おわりに

本稿では、SPECTの標準化に関して、著者らの最近の取り組みを含めて概説した。本稿で紹介したQSPECTパッケージは、まだ発展途上であり、今後もSPECTの標準化を見据えて、さらなる発展が期待される。

文 献

- [1] PET・PET/CT・サイクロトロン設置予定施設一覧。月刊新医療。エム・イー振興協会、東京、2007、pp79-82
- [2] SPECT設置機関名簿。月刊新医療。エム・イー振興協会、東京、2007、pp182-189
- [3] Zeniya T, Watabe H, Aoi T et al: A new reconstruction strategy for image improvement in pinhole SPECT. Eur J Nucl Med Mol Imaging 31: 1166-1172, 2004
- [4] Hapdey S, Soret M, Ferrer L et al: Quantification in SPECT: myth or reality? a multi-centric study. IEEE Nucl Sci Symp Conf Record 5: 3170-3173, 2004
- [5] Hudson H, Larkin R: Accelerated image reconstruction using ordered subsets of projection data. IEEE Trans Med Imag: 100-108, 1994
- [6] Meikle S, Hutton B, Bailey D: A transmission-dependent method for scatter correction in SPECT. J Nucl Med 35: 360-367, 1994
- [7] Narita Y, Eberl S, Iida H et al: Monte Carlo and experimental evaluation of accuracy and noise properties of two scatter correction methods for SPECT. Phys Med Biol 41: 2481-2496, 1996
- [8] Kim K, Watabe H, Hayashi T et al: Quantitative mapping of basal and vasoreactive cerebral blood flow using split-dose (123)I-iodoamphetamine and single photon emission computed tomography. Neuroimage 33: 1126-1135, 2006
- [9] Deloar H, Watabe H, Kim K et al: Optimization of the width of the photopeak energy window in the TDCS technique for scatter correction in quantitative SPECT. IEEE Trans Nucl Sci 51: 625-630, 2004
- [10] Narita Y, Iida H, Eberl S et al: Monte Carlo evaluation of accuracy and noise properties of and noise properties of two scatter correction methods for 201TI cardiac SPECT. IEEE Trans Nucl Sci 44: 2465-2472, 1997
- [11] Kim K, Watabe H, Shidahara M et al: SPECT collimator dependency of scatter and validation of transmission-dependent scatter compensation methodologies. IEEE Trans Nucl Sci 48: 689-696, 2001
- [12] Watabe H, Ikoma Y, Kimura Y et al: PET kinetic analysis-compartmental model. Ann Nucl Med 20: 583-589, 2006



渡部浩司 (わたべ ひろし)

1995年東北大学大学院工学科卒業、博士(工学)。1993年英国ハマスミス病院MRCサイクロトロンユニット、1997-1999年米国NIH PET部門に留学。1995年より国立循環器病センター研究所勤務。専門はPET/SPECT関連したトレーサー動態解析画像処理。2004年より国立循環器病センター研究所内に先進工学センターが設立。分子イメージング関連の研究に従事する。

* * *

基礎医学

「再生医療における工学技術」

国立循環器病センター研究所 生体工学部

山岡 哲二

I. はじめに

近年、ES細胞やさまざまな組織幹細胞の単離が続いて、iPS細胞の作製も報告され、その分化や増殖に関する生化学的・細胞生物学的、あるいは、分子生物学的進歩はめざましい。一方、これらの有用細胞を如何にして組織や臓器へと導くか、あるいは、安全性が担保された臨床システムとして構築するかなど、再生医療における工学サイドのブレークスルーが急務である。

II. 再生医療

1988年、米国のシンポジウムのタイトルとしてTissue Engineering (組織工学) という用語が初めて使用された¹⁾。自然治癒が不可能なほど大きな損傷を受けた組織や臓器を修復する試みは古くから行われているが、従来の人工臓器では、材料に対する生体反応の制御が不十分なために長期の機能代替は困難であり、また、臓器移植では、ドナーの不足や免疫応答による拒絶反応に加えて倫理的問題が残っている。そこで、組織工学の検討が始まり、1993年、R. Langerらは、スキヤホールド(Scaffold, 足場材料)と呼ばれたポリグリコール酸(PGA)の不織布に軟骨細胞を播種してヌードマウスの皮下に埋入することで、異所的な軟骨の再生が誘導できること、さらに、この手法が、肝臓、腸、尿管、骨などへ展開できる可能性を示唆した²⁾。再生が困難と考えられていた軟骨組織を対象にしたことや、異所的な組織の再構築に成功したことで、世界的に組織工学が注目を集めた。1996年以降、我が国では“再生医工学”という領域として発展した。最近では、その訳語である“Regenerative Medicine”が、海

外でも一般的な用語となっている。

実は、このような、マトリックと細胞とを融合させるアイデアは、1980年頃から皮膚組織の再建をターゲットにして検討されていた。フィーダーレイヤー(Feeder Layer)なる細胞層の上で表皮組織が重層化することを利用して表皮シートが作製され、続いて、真皮の再生や、コラーゲンゲルと線維芽細胞、表皮細胞を組み合わせた皮膚の再生が相次いで報告された。その後、上述の軟骨再生へと展開され、さらに1988年には、ヒト胚性幹細胞の単離が報告され³⁾、その後も続々と組織幹細胞が、そして、最近、ヒトiPS細胞の作製が報告されるなど、組織工学の最大の問題であった有用細胞の入手問題が解決するとの期待がふくらみ、さらに精力的な研究が進められている。

ますます広がる再生医療研究を内容的に整理すると図1ようになる。まず、再生医工学と細胞移植に大別される。再生医工学の中心は、生分解性マトリックス(スキヤホールド)に細胞を播種して組織再生を狙うタイプの戦略である(図1-②, ③)。

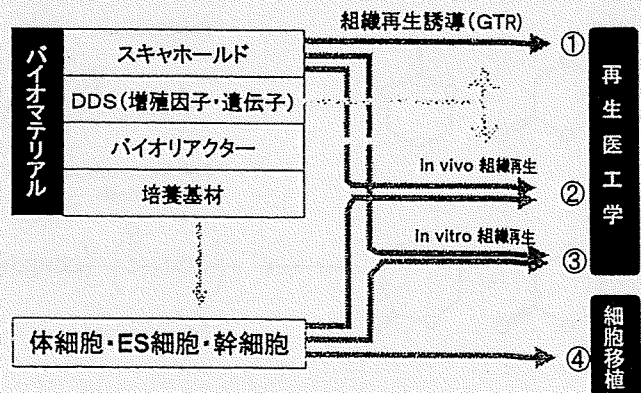


図1 再生医療の戦略

上述の例では、スキャホールドとして、PGA 不織布やコラーゲン多孔質体が使われた。これに対して、より古くから研究されていた図1の①は、スキャホールドのみを使って、*in vivo* で、組織再生を試みる戦略であり、組織再生誘導法 (GTR, Guided Tissue Regeneration) と呼ばれる。例えば図2のように、断裂した末梢神経を生体吸収性チューブでつなぐことで、ある期間、末梢神経が再生する空間を確保することが目的である。その他、GTRは、歯

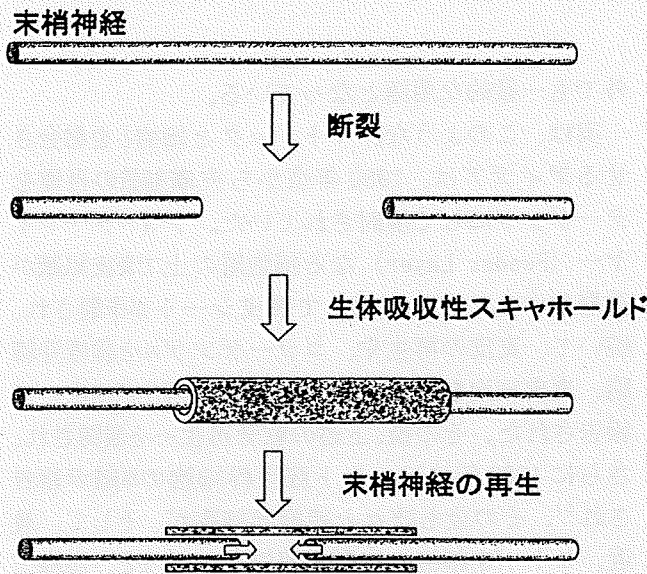
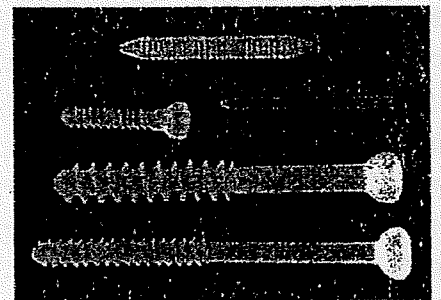
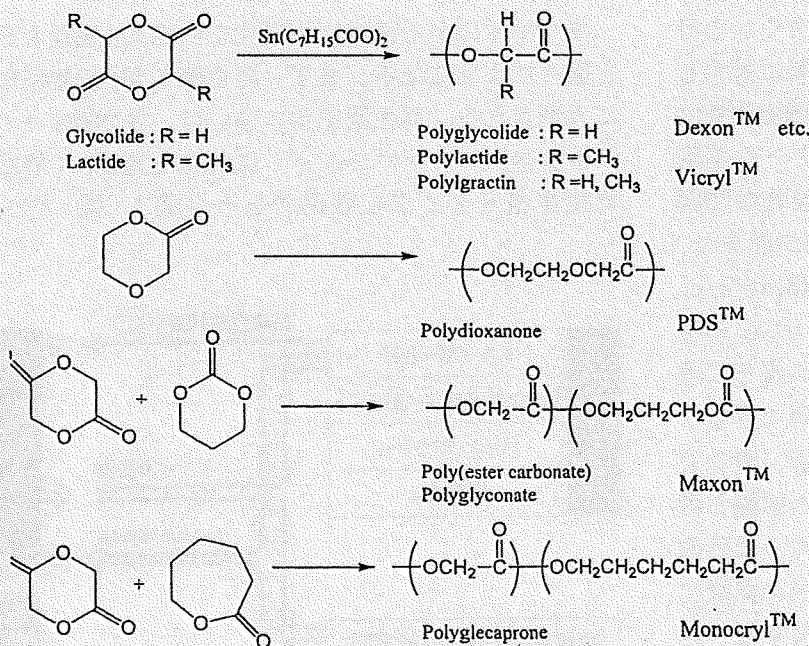


図2 GTRによる組織再生

周組織や顎堤への検討が進んでいる。また、図1の④に示した細胞移植は、マトリックスを利用することなく、幹細胞や体細胞などを欠損部位に注入する方法である。臨床という意味で最も進んでいるのが、この細胞移植ではないだろうか。特に自己幹細胞を移植することによる心疾患⁴⁾やパーキンソン病⁵⁾の治療において優れた効果が報告されている。これらの先進的手法が、一般的な治療法となるには解決しなくてはならない課題もまだまだ多い。我々は、再生医療を支援するあらゆる工学技術の開発を目指して、PLAを一成分とする共重合体からなる機能性スキャホールドの開発、*in vitro* 組織再生を進める新規バイオリクターの設計開発、細胞の移植効率を向上させるインジェクタブルスキャホールドの開発、さらには、移植細胞を生体内で追跡する分子イメージングシステムの構築などを進めてきた。

III. ポリ乳酸の化学修飾(柔軟性と細胞特異性)

初期の組織工学では、PGAやPLAなどからなる不織布が採用された。その役割は、文字通り“足場”としての機能であり、細胞が接着して増殖するための固相表面を提供することである。選択された最大の理由は、骨固定ピン^{6,7)}や外科用縫合糸として既に臨床の場で用いられ、歴史的にも安全性が確保されているためである(図3)^{8,9)}。図4には、代表的



↑骨固定ピン ↓縫合糸

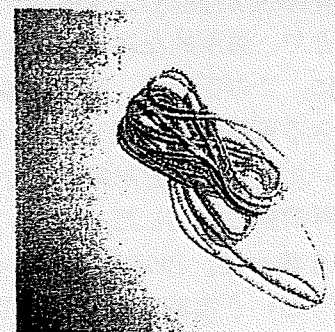


図3 医療用に用いられているポリ-α-ヒドロキシ酸

なランダム共重合体の分解速度を示した¹⁰⁾。分解はアモルファス領域から進むので、少量の他成分モノマーとの共重合により結晶化度が低下して分解速度が飛躍的に上昇する。一方、官能基を側鎖に有する環状モノマーとの開環共重合により、側鎖に官能

基を有するPGA 誘導体やPLA 誘導体を得られる。生体内に埋入されるPLA系材料には、高い組織親和性や細胞親和性などの生物学的表面特性が要求されることも多いが、側鎖に官能基をもたないPLAの表面修飾は容易ではない。そこで、官能基を有する生体吸収性PLA誘導体が精力的に研究された¹¹⁾。導入された官能基に対して、細胞特異的接着リガンドを固定化することで、固定化量に依存した優れた細胞親和性が達成できている¹²⁾。

このようなモノマー合成を伴うランダム共重合は、特別な合成施設と技術が要求されるため、さらに簡便な手法として、ラジカル反応法や表面加水分解法の開発が重要である¹³⁾。一方、造血幹細胞やEPCを用いた血管再生が期待され、モノクローナル抗体を用いた磁気ビーズ法や、蛍光剤を用いたFACS法により単離した細胞の利用が試みられているが、操作が困難であり、必ずしも臨床に適した方法ではない。そこで、造血幹細胞を選択的に吸着する生体吸収性スキャホールドに対して、採取した骨髓細胞を直接播種して移植できる治療システムの構築を目指した(図5)。すでに血管再生用スキャホールドとして用いられているポリ乳酸の多孔質体

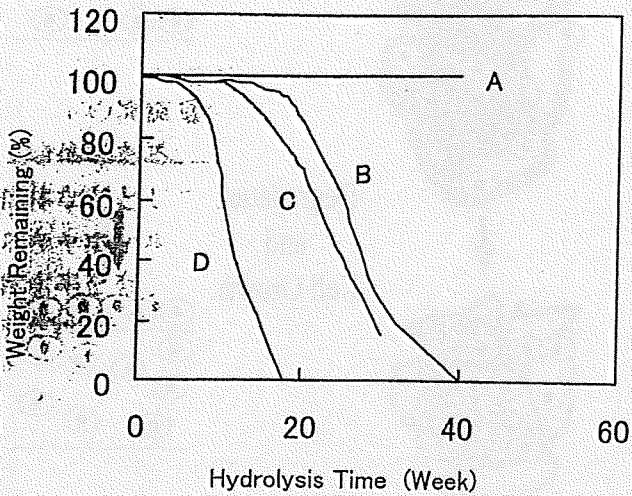


図4 ポリ乳酸誘導体の分解速度
(A) PLA, (B) PLA-co-ポリεカプロラクトン(50:50)⁺, (C) PLA-co-ポリεカプロラクトン(75:25), および (D) ポリグリコール酸

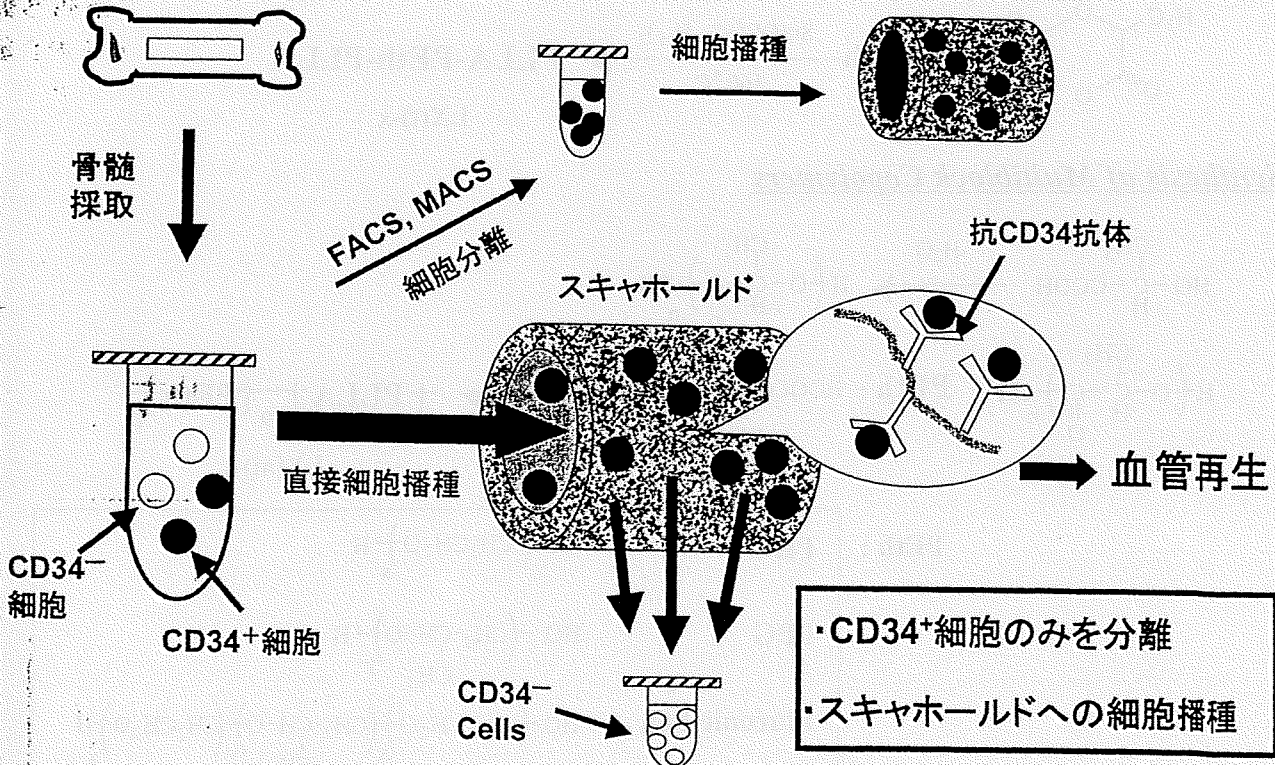


図5 幹細胞特異的抗体を表面に固定化した血管再建用スキャホールドは、骨髓細胞中のCD34陽性細胞のみをトラップする

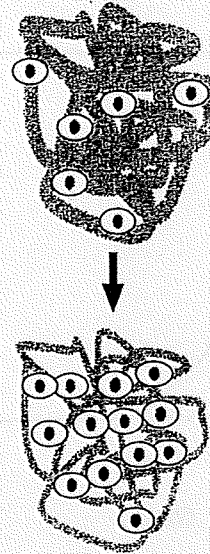
の表面を、所定濃度の NaOH で加水分解することで表面にカルボキシル基を導入し、カルボジイミド法により、抗 CD34 抗体を固定化した。この抗体修飾スキャホールド上に、CD34 陽性のモデル細胞 (KG-1a 細胞)、CD34 陰性のモデル細胞 (HL60)、および、イヌ骨髄細胞を約 2×10^6 個 / 50ml の濃度で、流速 0.05ml/min で播種し、接着した細胞数を WST-1 法により計数し、接着細胞種は、免疫染色にて評価した。抗体固定化スキャホールド上には、オリジナルスキャホールドに対して、約 4 倍の CD34 陽性細胞が吸着し、さらに、KG-1a 細胞と HL60 細胞の混合モデル細胞系では、80% 程度の CD34 陽性細胞濃縮効率が得られ、また、イヌ骨髄細胞播種システムに於いても、有意な CD34 陽性細胞の選択播種が確認された。現在、その効率を向上させるべく、抗体固定化濃度の向上と配向化を進めている。

IV. ポリ乳酸系含水ゲルの開発

PGA や PLA の多孔質体では疎水性が高いために水分を多く含む軟組織との親和性には問題がある。図 6 には、ポリ乳酸不織布を用いた場合と、コラーゲ

ンゲルを用いた場合の組織再生の違いについて示した。コラーゲンゲルは、軟組織との親和性が高いた

PLA or PGA (Guided Regeneration)



Collagen Gel (Active Regeneration)

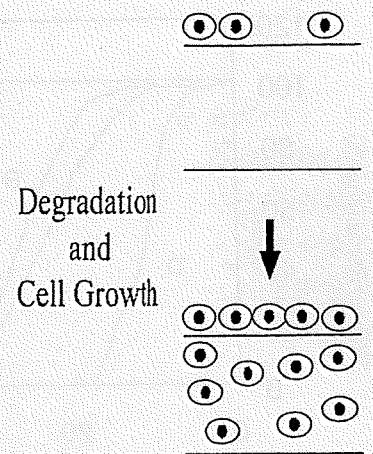
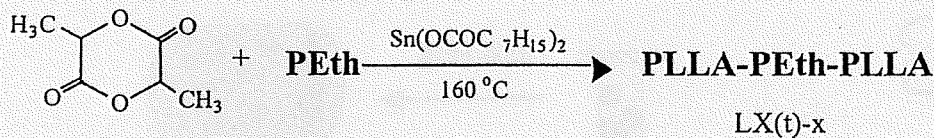
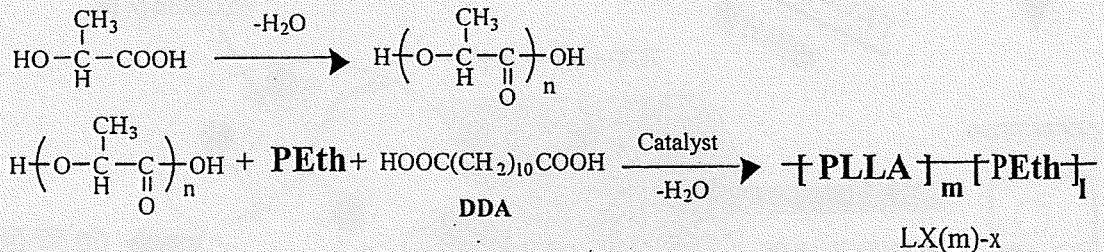


図 6 PLA などの疎水性の生体吸収性材料とコラーゲンゲルとではその組織再生機構が大きく異なる

Synthesis of Triblock Copolymers



Synthesis of Multiblock Copolymers



PEth :

PEG	$\text{HO} \left(\text{CH}_2\text{CH}_2\text{O} \right)_x \text{H}$
PPG	$\text{HO} \left(\text{CH}_2-\underset{\text{CH}_3}{\text{CH}}-\text{O} \right)_y \text{H}$
Pluronic F68	$\text{HO} \left(\text{CH}_2\text{CH}_2\text{O} \right)_x \left(\text{CH}_2-\underset{\text{CH}_3}{\text{CH}}-\text{O} \right)_y \left(\text{CH}_2\text{CH}_2\text{O} \right)_x \text{H}$

図 7 ポリ乳酸とポリエーテルからなるトリブロック、および、マルチブロック共重合体の合成方法

めに、周囲から積極的に細胞が浸潤して組織と置換される。それに対して、PLA などでは、非酵素的加水分解の結果生成した間隙で細胞が増殖する。我々は、ポリ乳酸と水溶性ポリエーテル (PEth) とのブロック共重合体を開発し、高親水性かつコラーゲンの様な軟組織再生を誘導する合成スキャホールドとして利用することを目的に開発を進めた¹⁴⁾。一般的には、従来の PLA/PEth ブロック共重合体は、図7に示した PEth 末端の水酸基を開始点とするラクチドの開環重合により合成されるトリブロック共重合体である。このトリブロック共重合体は、薬物担体などにおいては有用であるが、強度が要求される架橋構造には利用が困難である。高強度で高含水率を有する共重合体には以下の3つの条件が要求される。

- 十分な力学的強度を得るためには、100,000 程度の分子量が必要。
- PEth の分子量が、腎臓から排泄される 20,000 程度以下であることが必要。
- 十分な含水性を達成するためには、数十%以上の PEth 組成が必要。

これら3つの条件を満たす共重合体は、トリブロック体では合成が不可能であり、(AB)_n型マルチブロック共重合体が必須である。そこで、オリゴ乳酸と PEth の直接縮合反応によりマルチブロック共重合体を開発した(図7)。所定量のデカンジカルボン酸を系中の水酸基とカルボキシル基を等モル量に調節するために添加し、さらに、ジフェニルエーテルを溶媒とした環流により脱水重縮合を加速させる。PEth 組成の上昇と共に共重合体の分子量が低下するトリブロック共重合体とは異なり、マルチブロック共重合体では、PEth 組成に関係なく分子量

100,000 以上を実現することに成功した。その結果、速い分解速度と親水性表面を有しながらも十分な初期破断強度を有する繊維、メッシュ、フィルム、不織布、スポンジなどを調製することが可能となった。このマルチブロック共重合体は、PEth 組成の上昇とともに、含水率が上昇し、ラット皮下に埋入実験において、ほとんどカプセル化も認められず、炎症反応も軽微であった¹⁵⁾。これらの含水性マルチブロック共重合体をベースにして作製した、組織誘導性スキャホールドによる皮膚組織再生においては、スキャホールド内での毛細血管網構築性が確認されている(図8)。

V. 細胞移植を支援するインジェクタブルスキャホールド

上述の如く、臨床化が大いに期待される幹細胞移

新生血管

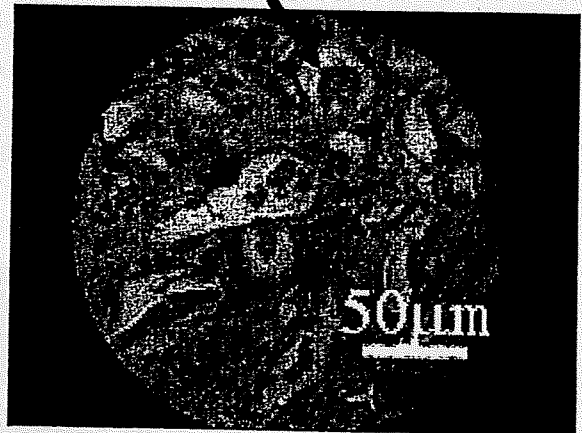


図8 マルチブロック共重合体をベースにしたスキャホールド内への血管新生

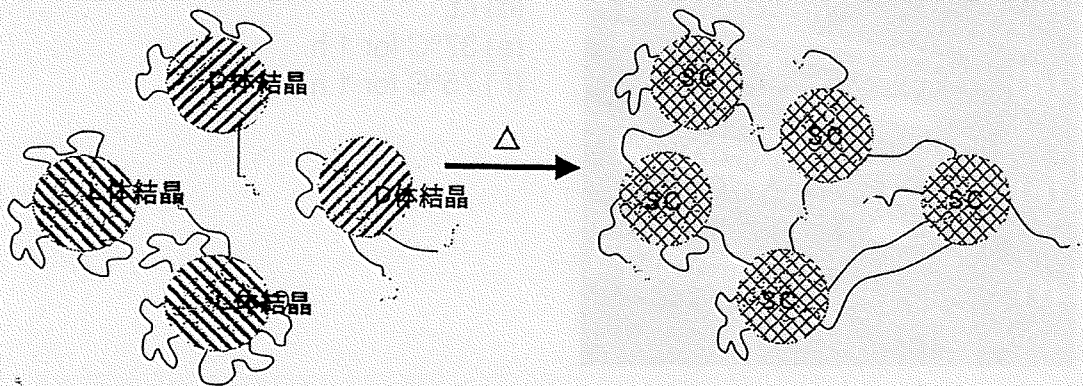


図9 L体ミセル/D体ミセル混合溶液の温度応答性ゲル化メカニズム

植術であるが、まだまだ、問題も多い。例えば、細胞懸濁液を直接組織などに注入した場合には、細胞を効率よく患部に留められない。そこで、細胞注入を支援する材料として、体内で、水溶液から含水ゲルへ変化する生体吸収性材料（インジェクタブルスキャホールド）が注目されている。従来から、光反応性基や、化学反応性基、あるいは、ポリ（N-イソプロピルアクリルアミド）などの温度応答性ポリマーが利用されたが、いずれも、その生体内での安全性は確保されていない。我々は、PLA とポリエチレングリコール（PEG）という、生体内での利用実績に優れた2つの高分子材料のみを利用することで、温度応答性を実現させインジェクタブルスキャホールドとすることに成功した。

京都工芸繊維大学木村良晴教授らとの共同研究の中で、いろいろなミセルをAFMで観察していた時、ある条件を満たしたミセルが、加熱処理によってナノ繊維構造に変化することを、偶然、見いだした¹⁶⁾。ミセルからナノ繊維への変化には、隣接するミセル同士が相互作用（コアを形成するポリ乳酸部分が、コロナ構造を形成するPEG層を乗り越えて融合）する必要がある。そこで、ポリ-L-乳酸からなるミセル（L体ミセル）と、ポリ-D-乳酸からなるミセル（D体ミセル）の分散液を混合することを発案し

た（図9左）。というのも、加熱により隣接するL体ミセルとD体ミセルが融合すると、ステレオコンプレックスミセルが形成し、その結果、図9右に示すように3次元架橋構造が成長してゲル化するというアイデアである。ポリ乳酸のステレオコンプレックスは、ホモ結晶に比べて融点が約50°Cも高い安定な構造であることも、ゲル化を促進して安定化することに寄与すると考えられる。実際に、共重合結

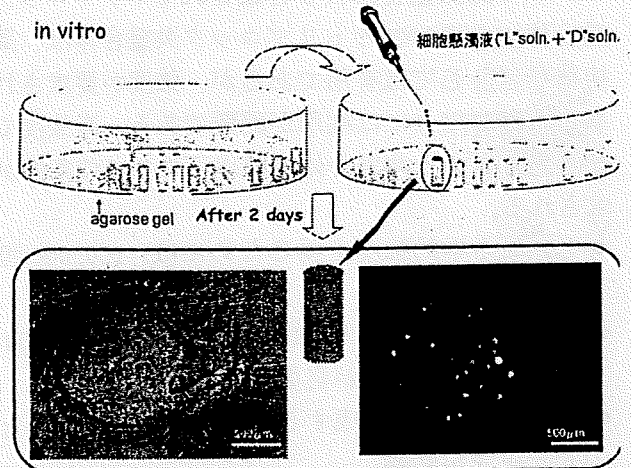


図11 L体ミセル・D体ミセル混合液に対して、GFP；伝子組み換え細胞を混合し、in vitro でゲルさせることで、このゲル内での細胞生存性が確認された。

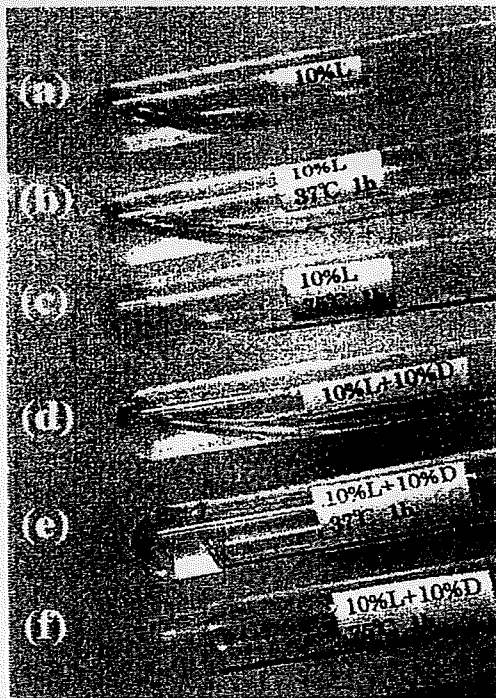


図10 L体ミセルとD体ミセル混合液（d）は、37度に加温することで透明なゲルに転移する（e）。それに対して、L体ミセルのみの分散液（a）は75度で白濁はするがゲル化には至らない。

The aqueous dispersion (10wt%) of PLLA-PEG-PLLA (1300-4600-1300)
 (a) r.t.
 (b) 37°C for 1 h
 (c) 75°C for 1 h
 The mixture of each dispersion (10wt%) of PLLA-PEG-PLLA (1300-4600-1300) and PDLA-PEG-PDLA (1100-4600-1100)
 (d) r.t.
 (e) 37°C for 1 h
 (f) 75°C for 1 h

成などを調節して37°Cでゲル化することに成功したインジェクタブルスキャホールドの写真を図10に示した。X線散乱測定により、温度上昇とともにステレオコンプレックス結晶が成長することがそのメカニズムであることも証明された。得られたゲルの含水率は90%以上であり、その物質透過性に優れること、さらに、細胞毒性を誘発する一切の化学物質を利用していないために、細胞生存率を下げることなく、対象部位に細胞を注入できる材料となる。図11は、このことを示す*in vitro* 実験の結果である。澁谷ミセル液にGFP(緑色蛍光タンパク)組換えマウス胎児線維芽細胞を懸濁させて、アガロースゲル中で昇温ゲル化させた3日後にも、細胞は正常な移動とGFP発現機能を維持する。

VI. 細胞トラッキング

細胞移植療法のもう一つの大きな課題は、その治療メカニズムが未だ不明なことである。すなわち、組織再生や機能改善が、移植した細胞自身の増殖により機能が回復したためによるのか、あるいは、移植した細胞が産生する生理活性物質などに対してレシピエント(移植を受けた患者)が反応することで

治癒したパラクライン効果によるものかを解明する手だてがない。特に、自家細胞移植では免疫染色で移植した細胞を区別することさえも困難である。一つの手法として、GFP(+)の細胞をGFP(-)マウスに移植して*in vivo* 蛍光イメージング装置で追跡する手法があるが、蛍光の特性により、ラット程度の小動物が限界である。最近、我々は、移植した細胞をMRIで低侵襲的に追跡するための、新たな細胞標識用MRI造影剤の開発に成功した。この目的を達成するには、磁性を有する分子(ガドリニウム錯体など)を移植細胞の細胞質内に長期間安定に滞留させる技術が必須となる。さらに、細胞の増殖や機能発現を妨げることなく、細胞が死滅したときには、この造影剤が速やかに体外へ排泄されることが必要である。図12に、本システムの概要を示した。ガドリニウム錯体分子(丸印)の細胞膜透過性を抑制し、かつ、細胞に対する毒性を軽減させるために高分子キャリアを用いた。この高分子化造影剤は、微弱な電氣的ショックを細胞に加える手法により、あらゆる細胞に対して容易に送達することができる¹⁷⁾。NIH3T3細胞、および、ラット間葉系幹細胞を、本造影剤にて標識したところ、その細胞増殖性は、10

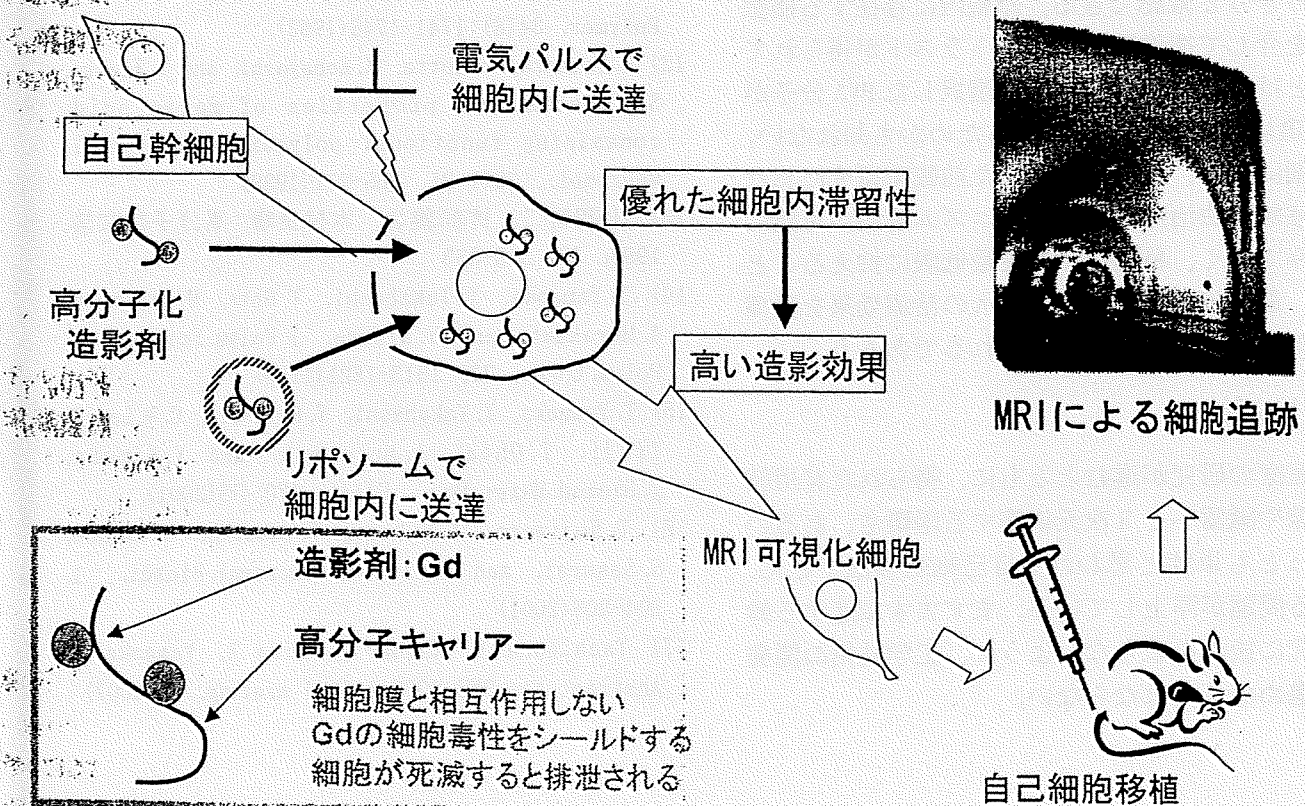


図12 移植した自己幹細胞をMRIにより追跡するための高分子化MRI造影剤システム

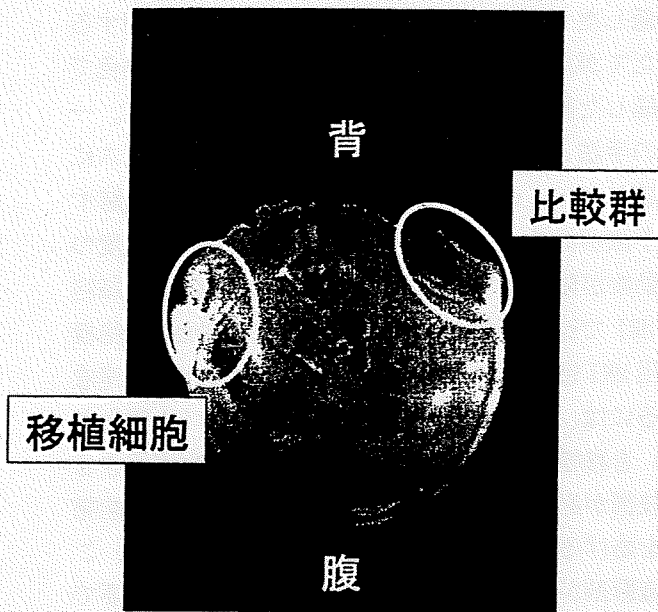


図13 高分子化MRI造影剤を封入した細胞を皮下に移植したマウスのMRI断層写真

日間にわたって、細胞からの造影剤の有意な漏出は認められなかった。このことより、1年程度は、移植細胞をMRIにより追跡できる性能を有していると考えられる。図13は、標識したNIH3T3細胞を皮下に埋入したマウスの、MRI断層写真である。移植細胞がはっきりと確認できる。細胞内に存在する極微量の水を介して撮像可能なコントラストが得られていることは、キャリアーとして選択したPVA分子がGd周囲環境の水を確保しているためかも知れない。本造影剤により、大動物を用いた前臨床研究における細胞移植療法治療効果のメカニズム解明が可能になるのみでなく、移植細胞数を最低限に抑えることにより、最低限のリスクで、最大の治療効果を発揮させるための定量的指標を得られるであろう。

VI. さいごに

再生医療の研究が進むとともに、得られた有用細胞を組織や臓器へと3次元構築する困難さ、あるいは、もっとも単純と思われる自己細胞移植でさえ、あらゆる問題が浮上している。ますます加速する幹細胞研究に後れを取らないように、工学技術の開発研究を進めなくてはならない。

●参考文献

- 1) “再生医工学”、筏義人編、化学同人(2001)
- 2) R. Langer and J. P. Vacanti, Science, 260, 920-924 (1993)
- 3) J. A. Thomson, J. Itskovitz-Eldor, S. S. Shapiro, M. A. Waknitz, J. J. Swiergiel, V. S. Marshall, J. M. Jones, Science, 282, 1145(1998)
- 4) Y. Miyahara, N. Nagaya, M. Kataoka, B. Yanagawa, K. Tanaka, H. Hao, K. Ishino, H. Ishida, T. Shimizu, K. Kangawa, S. Sano, T. Okano, S. Kitamura, H. Mori, Nat. Med., 12(4), 459(2006)
- 5) S. W. Kim, H. Han, G. T. Chae, S. H. Lee, S. Bo, J. H. Yoon, Y. S. Lee, K. S. Lee, H. K. Park, K. S. Kang, Stem Cell, 24, 1620(2006)
- 6) J. Mauduit, E. Perous, M. Vert, J Biomed Mater Res, 30, 201-207(1996)
- 7) Y. Ikada, Y. Shikinami, Y. Hara, M. Tagawa, E. Fukada, J Biomed Mater Res, 30:553-558(1996).
- 8) R. E. Johnson, J. A. Lanaski, V. Gupta, M. J. Griffen, H. T. Gaud, T. E. Needham, H. Zia, J Controlled Release, 17:61-67(1991).
- 9) N. Nihant, C. Schugens, C. Grandfils, R. Jerome, R. Teyssie, Pharm Res, 11:1479-1484(1994).
- 10) A. Echeverria J. Jimenez, Surgery, 131, 1-13 (1970).
- 11) Y. Kimura, K. Shirota, H. Yamane, T. Kitao, Polymer, 34(8):1741-1748(1993).
- 12) T. Yamaoka, Y. Hotta, K. Kobayashi, and Y. Kimura, Synthesis and properties of malic acid-containing functional polymers, Int. J. Biol. Macromol., 25(1-3), 265-271(1999)
- 13) 山岡哲二、竹部義之、木村良晴：高分子論文集、1998, 55, 328-333
- 14) T. Yamaoka, Y. Takahashi, T. Ohta, M. Miyamoto, A. Murakami, and Y. Kimura, J. Polym. Sci. Part A: Polym. Chem., 37, 1513-1521(1999)
- 15) T. Yamaoka, Y. Takahashi, T. Fujisato, C. W. Lee, T. Tsuji, T. Ohta, A. Murakami, and Y. Kimura, J. Biomed. Mater. Res., 54(4), 470-479(2001)
- 16) T. Fujiwara, T. Mukose, T. Yamaoka, H. Yamane, S. Sakurai, and Y. Kimura, Macromol. Biosci., 1, 204-208(2001)
- 17) Tachibana Y, Ennmi J, Iida H, Yamaoka T, Abstract for SFB 2007 Annual meeting, 94(2007)

Absolute quantitation of myocardial blood flow with ^{201}Tl and dynamic SPECT in canine: optimisation and validation of kinetic modelling

Hidehiro Iida · Stefan Eberl · Kyeong-Min Kim ·
Yoshikazu Tamura · Yukihiko Ono ·
Mayumi Nakazawa · Antti Sohlberg · Tsutomu Zeniya ·
Takuya Hayashi · Hiroshi Watabe

Received: 18 September 2007 / Accepted: 4 November 2007
© Springer-Verlag 2007

Abstract

Purpose ^{201}Tl has been extensively used for myocardial perfusion and viability assessment. Unlike $^{99\text{m}}\text{Tc}$ -labelled agents, such as $^{99\text{m}}\text{Tc}$ -sestamibi and $^{99\text{m}}\text{Tc}$ -tetrofosmine, the regional concentration of ^{201}Tl varies with time. This study is intended to validate a kinetic modelling approach for in vivo quantitative estimation of regional myocardial blood flow (MBF) and volume of distribution of ^{201}Tl using dynamic SPECT.

Methods Dynamic SPECT was carried out on 20 normal canines after the intravenous administration of ^{201}Tl using a commercial SPECT system. Seven animals were studied at

rest, nine during adenosine infusion, and four after beta-blocker administration. Quantitative images were reconstructed with a previously validated technique, employing OS-EM with attenuation-correction, and transmission-dependent convolution subtraction scatter correction. Measured regional time-activity curves in myocardial segments were fitted to two- and three-compartment models. Regional MBF was defined as the influx rate constant (K_1) with corrections for the partial volume effect, haematocrit and limited first-pass extraction fraction, and was compared with that determined from radio-labelled microspheres experiments.

Results Regional time-activity curves responded well to pharmacological stress. Quantitative MBF values were higher with adenosine and decreased after beta-blocker compared to a resting condition. MBFs obtained with SPECT ($\text{MBF}_{\text{SPECT}}$) correlated well with the MBF values obtained by the radio-labelled microspheres (MBF_{MS}) ($\text{MBF}_{\text{SPECT}} = -0.067 + 1.042 \times \text{MBF}_{\text{MS}}$, $p < 0.001$). The three-compartment model provided better fit than the two-compartment model, but the difference in MBF values between the two methods was small and could be accounted for with a simple linear regression.

Conclusion Absolute quantitation of regional MBF, for a wide physiological flow range, appears to be feasible using ^{201}Tl and dynamic SPECT.

H. Iida (✉) · S. Eberl · K.-M. Kim · M. Nakazawa ·
A. Sohlberg · T. Zeniya · T. Hayashi · H. Watabe
Department of Investigative Radiology,
National Cardiovascular Center Research Institute,
Fujishiro-dai,
Suita City, Osaka 565-8565, Japan
e-mail: iida@ri.ncvc.go.jp

S. Eberl
PET and Nuclear Medicine Department,
Royal Prince Alfred Hospital,
Missenden Road,
Camperdown, NSW 2050, Australia

Y. Tamura
Department of Cardiology, Akita Kumiai General Hospital,
1-1-1, Nishi-bukuro, Iijima,
Akita City 011-0948, Japan

Y. Ono
Akita Research Institute of Brain,
6-10, Senshu-Kubota Machi,
Akita City 010-0874, Japan

Keywords Myocardial blood flow · Dynamic SPECT ·
Thallium-201 · Compartment model · Quantitation

Introduction

Myocardial perfusion imaging using Thallium-201 (^{201}Tl) is well established in routine clinical practice for detecting

exercise-induced myocardial ischaemia and/or for assessing myocardial viability in patients with coronary artery disease. The diagnosis, however, has been limited to qualitative or visual assessment of the physical extent of the defect areas rather than quantitative assessment of physiological functions. Quantitative methods would for example enable longitudinal studies when assessing therapy response and pharmacological interventions. Some groups have already investigated the feasibility of estimating quantitative parameters with dynamic SPECT in the myocardium using ^{201}Tl [1] and $^{99\text{m}}\text{Tc}$ -Teboroxime [1, 2], but these techniques have not yet been applied to clinical practice. This is largely attributed to the fact that quantitative reconstruction programmes are not readily available on commercial SPECT systems.

We have developed a reconstruction programme package for SPECT, which can accurately provide quantitative images of radio-labelled tracer distributions *in vivo*, which is a pre-requisite for absolute physiological parameter estimation. The adequacy and accuracy of these methods have been demonstrated in multiple papers for $^{99\text{m}}\text{Tc}$ and ^{201}Tl in cardiac studies [3–5], and for $^{99\text{m}}\text{Tc}$ and ^{123}I in brain studies [6]. It has also been demonstrated, in brain studies, that physiological parameters such as cerebral perfusion [6] and cerebral flow reactivity [7] obtained using our package were as accurate as those determined by PET. These findings suggest that absolute quantitation of regional myocardial perfusion might also be possible in a clinical setting using commercial SPECT cameras.

^{201}Tl is a potassium analogue, and its kinetics has been extensively investigated in previous studies [8, 9]. Due to the high first-pass extraction fraction (EF) [10] and a large distribution volume, ^{201}Tl has been considered an ideal tracer for quantitation of absolute myocardial blood flow, not only at rest but also at hyperemic conditions. As a clinical implication, quantitative assessment of MBF and coronary flow reserve is important. For instance, coronary microvascular dysfunction or impaired endothelial function in patients with coronary risk factors or patients with cardiomyopathy or with heart failure is an un-resolved important issue to answer [11]. Coronary flow reserve can also be reduced in patients with hyper-cholesterolemia without overt coronary stenosis [12]. The low energy and long half-life of ^{201}Tl have, however, seriously limited its use in nuclear cardiology.

The goal of this study was to validate our reconstruction methodology for the estimation of myocardial blood flow using ^{201}Tl and dynamic SPECT using tissue time-activity curves (TTAC) derived from myocardial regions. In addition, we aimed to find the optimal kinetic model configuration and to investigate the factors affecting the estimation of physiological parameters such as the partial volume effect (PVE), appropriate choice of input function, conversion from plasma to blood flow using haematocrit (Hct) and the limited first-pass tracer EF.

Materials and methods

Subjects

A total of 21 dogs were studied in which 8 were in a resting condition, 9 dogs during constant infusion of adenosine for increased MBF, and 4 dogs during constant infusion of beta-blocker. Of the 21 studies, 1 study was un-successful and projection data could not be retrieved from the scanner, reducing the number of resting studies to 7 and total dog studies to 20. Adenosine was infused continuously over the study duration at a rate ranging from 140 to 700 mg/kg/h to achieve a range of blood flow increases. An initial dose of beta-blockers ranging from 2 to 6 mg was given, followed by a constant infusion for the duration of the study of 2 or 4 mg/h. The study protocol was approved by the animal ethics committee at the Akita Research Institute of Brain, Akita City, Japan where all experiments were carried out.

SPECT procedures

All dogs were anaesthetised, and the catheters for dose administration and arterial blood sampling were inserted before the study. The SPECT system was a conventional dual-head gamma camera (Toshiba GCA-7200A, Tokyo, Japan) fitted with short focal length fan-beam collimators (LEHR-Fan). The transverse field-of-view (FOV) was 22 cm diameter and axial FOV was 20 cm. The dogs were carefully taped into a cradle to minimise motion during the study, and also to ensure that no truncation occurred. Heart rate and blood pressure were monitored throughout the study and recorded at regular intervals.

Before the injection of any tracer, a 15-min transmission study was carried out in which a rod source filled with approximately 740 MBq of $^{99\text{m}}\text{Tc}$ was placed along the focal line of one of the fan-beam collimators (see Fig. 1). The transmission study was followed by injection of 3 MBq of ^{141}Ce microspheres into the left ventricle via a catheter and blood was withdrawn from the aorta at a constant flow rate of 5 ml/min for 2 min to serve as an input function. For the pharmacological intervention studies, adenosine infusion or beta-blocker injection followed by infusion was commenced before the ^{141}Ce microsphere administration.

Dynamic SPECT was commenced with the start of the 4-min constant infusion of 110 MBq ^{201}Tl . The frame collection rates and 360° rotation times were 10×1 min (rotation time 15 s), 6×2 min (30 s), 3×4 min (60 s) and 5×5 min (60 s) for the first hour for all studies. Resting blood flow studies had an additional 18×10 min (120 s) frames collected for a total study period over 4 h. The shorter total study time for the drug infusion studies was mandated by the difficulties in keeping the dogs stable with prolonged infusions of the drugs used. A 34% energy

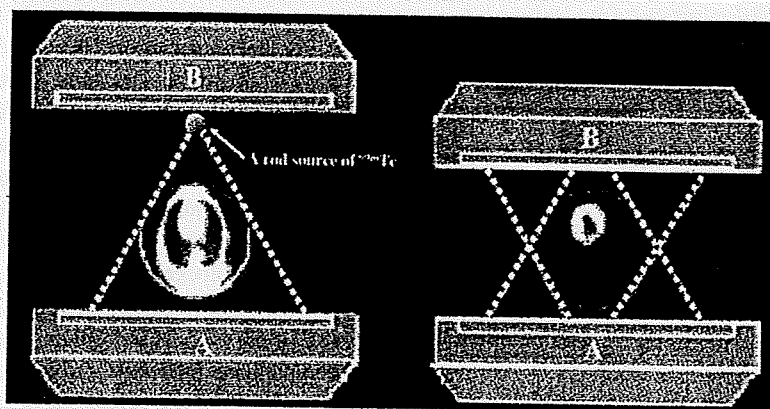


Fig. 1 Schematic diagram of data acquisition using a clinical dual-headed SPECT camera fitted with fan-beam collimators. Transmission scan was performed using a ^{99m}Tc -filled rod source placed at a focal

line of one of the collimators, and only one of the detectors was used (*left*). Both detectors were used in the emission scan (*right*)

window centred on 77 keV was used for the ^{201}Tl acquisitions [4, 13].

Arterial blood samples were taken every 20 s for the first 6 min, every 60 s for 6–10 min, 120 s for 10–20 min, 300 s for 20–30 min and 600 s for 30–60 min. For the resting studies, blood samples were also taken every 20 min for 1–2 h and additional samples at 2.5, 3 and 4 h post- ^{201}Tl infusion. In six studies, plasma was separated immediately after sampling by centrifugation, and plasma samples were counted in a well counter cross-calibrated with the SPECT scanner. To minimise the effects of the continued exchange of ^{201}Tl between plasma and red blood cells in the test tubes after sampling, immediate, rapid separation of plasma from whole blood was required. An averaged relationship between plasma and whole blood concentration ratio over time was obtained, and then multiplied with the whole blood curves for all studies to derive a plasma input function.

At the end of the SPECT study, the microsphere blood flow measurement was repeated with ^{51}Cr microspheres. The dogs were then killed by injection of potassium chloride (KCl) and the myocardium was dissected into samples suitable for counting in the well counter. The ^{201}Tl concentration in the tissue samples was derived from the sample weight normalised gamma counter counts. The samples were stored to allow for the decay of ^{201}Tl ($T_{1/2} = 73$ h vs $T_{1/2} = 32.5$ days for ^{141}Ce and 27.8 days for ^{51}Cr) and then counted to measure the ^{141}Ce and ^{51}Cr activities. Separation between ^{141}Ce and ^{51}Cr counts was based on their respective gamma ray energies (145 keV for ^{141}Ce and 323 keV for ^{51}Cr).

SPECT data processing

Projection data were processed according to previously described procedures [5]. Briefly, the transmission data obtained by the fan-beam collimator were first re-binned

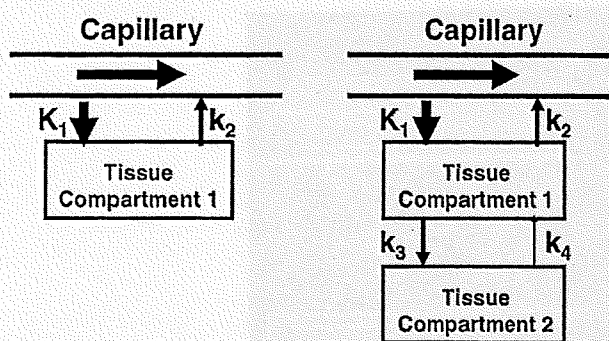
into parallel projections. Transmission projections were normalised by blank projection, re-constructed to generate quantitative maps of the attenuation coefficient for ^{99m}Tc and then linearly scaled to provide attenuation correction maps for ^{201}Tl . Emission data were corrected for detector non-uniformity and also re-binned into parallel projections. The projection data were then corrected for scatter with transmission-dependent convolution subtraction (TDCS) originally proposed by Meikle et al. [14] and further optimised by our group [4, 5]. The emission projection data were re-constructed with the OS-EM reconstruction algorithm [15] using three iterations and ten subsets. The re-constructed images were cross-calibrated with the well counter system.

Data analysis

Re-constructed images were normalised by acquisition time for each frame. Multiple circular regions of interest (ROI) were drawn on the myocardium, and the TTAC of ^{201}Tl were generated for the anterior, apical, lateral, posterior and septal areas of the myocardium. The two-compartment model (one tissue compartment) and three-compartment model (two tissue compartments) shown in Fig. 2 were applied to determine two parameters (K_1 and K_2) for the two-compartment model and four parameters (K_1 – K_4) for the three-compartment model by means of non-linear least squares fitting (NLLSF).

The regional MBF was considered to be related to K_1 obtained from compartment model fits. K_1 is, however, affected by the PVE, Hct and the limited first-pass EF whose effects were corrected according to Eq. 1:

$$\text{MBF} = \frac{\text{PVE}}{\text{EF} \times (1 - \text{Hct})} \times K_1 \quad (1)$$



2-Compartment model

3-Compartment model

Fig. 2 Two- and three-compartment models evaluated in this study. K_1 in units of ml/min/g denotes the regional MBF for both models. Distribution volume (V_d) in units of ml/g is defined as K_1/K_2 for the two-compartment mode, and $\frac{K_1}{k_2} \left(1 + \frac{k_3}{k_4}\right)$ for the three-compartment model

The physiological basis for the correction factors in Eq. 1 can be described as follows:

1. TTACs obtained from SPECT images are under-estimated due to the limited spatial resolution relative to the myocardial wall thickness and also due the myocardial contractile motion. This phenomenon is known as PVE. The PVE correction factor for each TTAC was determined from the ratio of the last SPECT frame counts to the ^{201}Tl myocardial tissue sample counts obtained from the tissue samples taken and measured with the well counter at the end of the SPECT scan.
2. The arterial input function for the compartment model studies was defined from the plasma radioactivity concentration curve, rather than the whole blood radioactivity curve. K_1 is therefore the regional "plasma" flow. Thus, for comparison with the microsphere flow measurements, which estimates the whole blood flow, K_1 was divided by $(1-\text{Hct})$ to obtain the flow for the total blood.
3. For a tracer with limited first-pass $\text{EF} < 1.0$, flow (MBF) is related to K_1 by $K_1 = \text{EF} \times \text{MBF}$. The first-pass EF is flow-dependent and decreases at high flow. We have applied an empirical formulation for the first-pass EF based on the data by Weich et al. [10] ($\text{EF} = 0.84 - 0.524 \cdot \log_{10}(K_1^*)$) where K_1^* is $K_1 / (1 - \text{Hct})$. The K_1 values obtained with two- and three-compartment models with/without corrections according to Eq. 1 were compared to the average of microsphere blood flow values obtained pre- and post-dynamic SPECT scan.

The distribution volume of ^{201}Tl (V_d) was defined as

$$V_d = \frac{K_1}{k_2} \text{ for the two-compartment model} \tag{2a}$$

$$V_d = \frac{K_1}{K_2} \left(1 + \frac{K_3}{K_4}\right) \text{ for the three-compartment model.} \tag{2b}$$

As mentioned before, the resting studies were collected for 4 h, whilst the adenosine and beta-blocker studies were collected for approximately 1 h. To investigate whether the shorter collection time introduces systematic bias, NLLSF fits restricted to the first 1 h of the resting study data were also performed and compared with the V_d values from the full 4 h resting data set and with the estimates obtained from the beta-blocker and adenosine studies.

Akaike information criterion (AIC) and Schwarz criterion (SC) were calculated for both two-compartment and three-compartment model fits [16] to test the adequacy of the two models. All data are presented as mean \pm 1 SD. Student's t test was employed in the comparison of the V_d values. Pearson's regression analysis was applied to compare K_1 and microsphere flow values. A probability value of < 0.05 was considered statistically significant.

Results

Figure 3 shows the plasma to whole blood concentration ratios in the six dogs with rapid plasma separation and the averaged data. Equilibrium is reached after about 40 min, at which time the mean ratio was found to be 0.76. As expected, relative plasma concentration is highest early on as the tracer is injected into the plasma (and not red blood cells). ^{201}Tl is rapidly cleared from the plasma causing a rapid decline in relative plasma concentration and "under-shoot" before equilibrium is established. Samples left for a prolonged period before plasma separation showed the value of approximately 0.78, which was close to the plasma to whole blood concentrations ratio at the equilibrium shown in

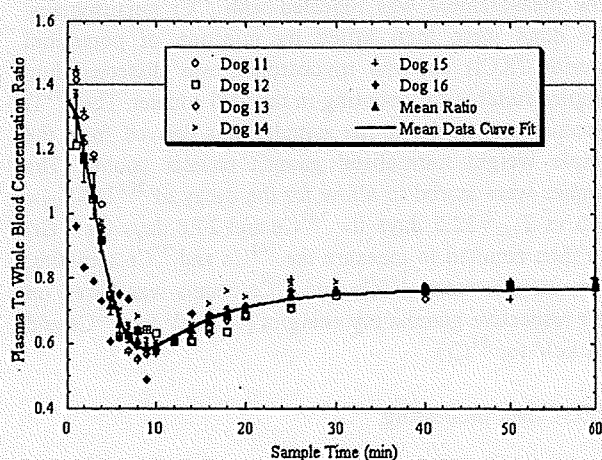


Fig. 3 Individual and mean plasma to whole blood concentration ratios over time for the six dogs with rapid plasma separation. Error bars indicate the standard error of the mean. Solid line is the curve fit to mean ratio data

Fig. 4 A typical example of sequential SPECT images of the myocardium for six representative slices after intravenous injection of ²⁰¹Tl into a canine at rest

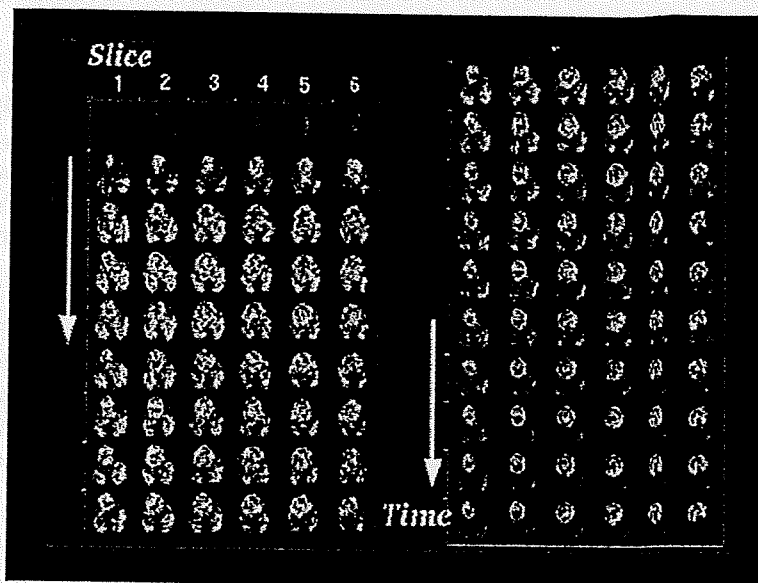


Fig. 3. The plasma to whole blood ratio curves could be approximated by the following equation:

$$R_{pl/wb} = A_0 e^{-\lambda(t+\Delta t)^2} + A_1 (1 - e^{-\lambda_2(t+\Delta t)}), \quad (3)$$

which resulted in $A_0 = 1.303 \pm 0.045$, $A_1 = 0.7649 \pm 0.0056$, $\lambda_1 = 0.03636 \pm 0.0039 \text{ min}^{-1}$, $\lambda_2 = 0.1263 \pm 0.0077 \text{ min}^{-1}$ and $\Delta t = 0.9516 \pm 0.41 \text{ min}$. The correlation coefficient for the fit was $r = 0.995$.

Figure 4 shows a typical example of sequential images after the intravenous injection of ²⁰¹Tl for six representative slices of a dog studied at rest. It can be seen that ²⁰¹Tl appeared in the ventricular chambers first and then gradually accumulated homogeneously into the left myocardium. The quality of these images is reasonably good, indicating that our approach of estimating the kinetic parameters by NLSF is feasible without excessive noise

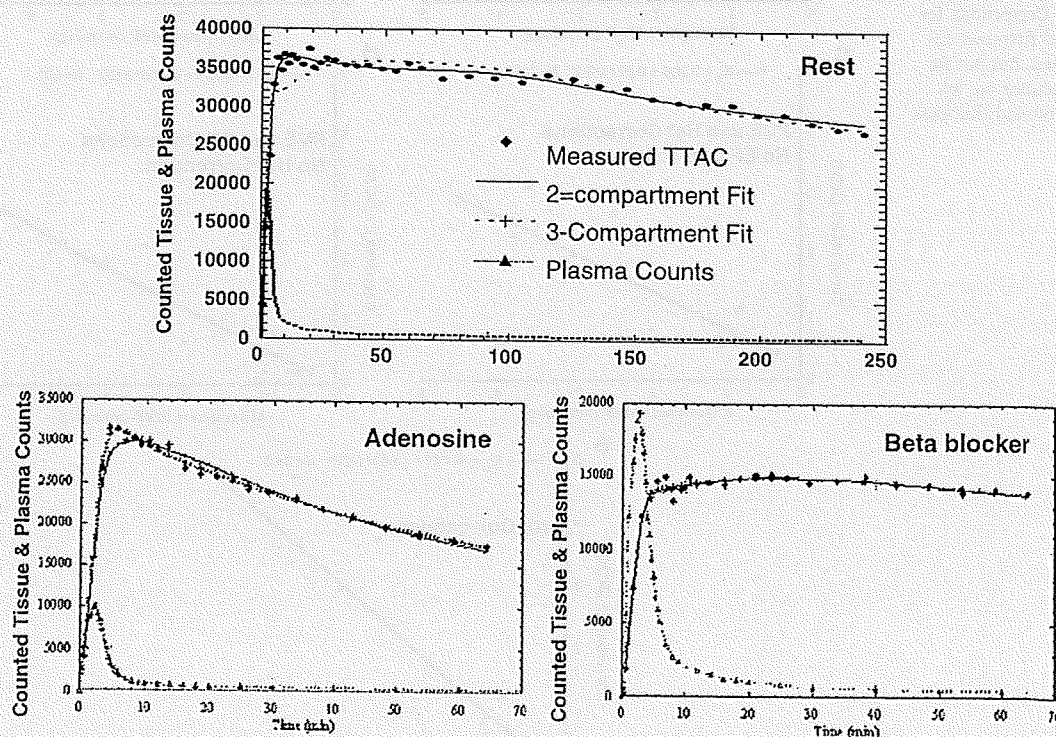


Fig. 5 TTACs and two- and three-compartment model fits for a resting, adenosine (increased MBF) and beta-blocker (reduced MBF) study. Note the different time scales for the resting study because

resting studies were collected for 4 h compared to ~1 h for the pharmacological intervention studies

amplification. Curve fits to representative TTACs for resting, beta-blocker and adenosine infusion studies are shown in Fig. 5. The height of the TTACs relative to the input function corresponded well with the pharmacological challenges. Compared to the resting studies, peaks of TTACs relative to the arterial input function were higher for adenosine and lower after beta-blocker administration. Results of kinetic fitting by the two- and three-compartment models are also plotted on this figure. Visually, the three-compartment model provided better fits than the two-compartment model to the observed TTACs, which is particularly evident for the initial scan period of the resting and adenosine studies.

Shown in Fig. 6a–e is the comparisons of K_1 obtained by NLLSF (three-compartment model fit) with the microsphere

flow estimates. Values were averaged over the myocardial segments in both axes, thus each point corresponds to a single study. There was good correlation between K_1 and the microsphere flow when no corrections were applied, but K_1 significantly under-estimated the true flow (Fig. 6a). All the corrections improved the K_1 estimates (Fig. 6b–d) and the best agreement between K_1 and microsphere flow was observed when all three factors were corrected as described in Eq. 1 (Fig. 6e). Results of the regression analysis also demonstrated the highest correlation coefficient when all three correction factors were applied. Table 1 summarises the results of the Akaike information criteria (AIC) and Schwartz criteria (SC) obtained from the kinetic fitting analysis for all myocardial segments of all subjects. Both

Fig. 6 Plot of K_1 derived from the three-compartment model fit against the mean of the pre- and post-dynamic SPECT microsphere blood flow measurements. **a** No correction for PVE, limited first-pass EF or conversion from plasma to blood flow has been applied. **b** Correction for PVE has been applied, but not for Hct or limited first-pass EF. **c** Corrections for PVE and Hct have been applied, but not for limited first-pass EF. **d** Corrections for PVE and limited first-pass EF have been applied, but not for Hct. **e** All corrections are applied for PVE, limited first-pass EF and Hct

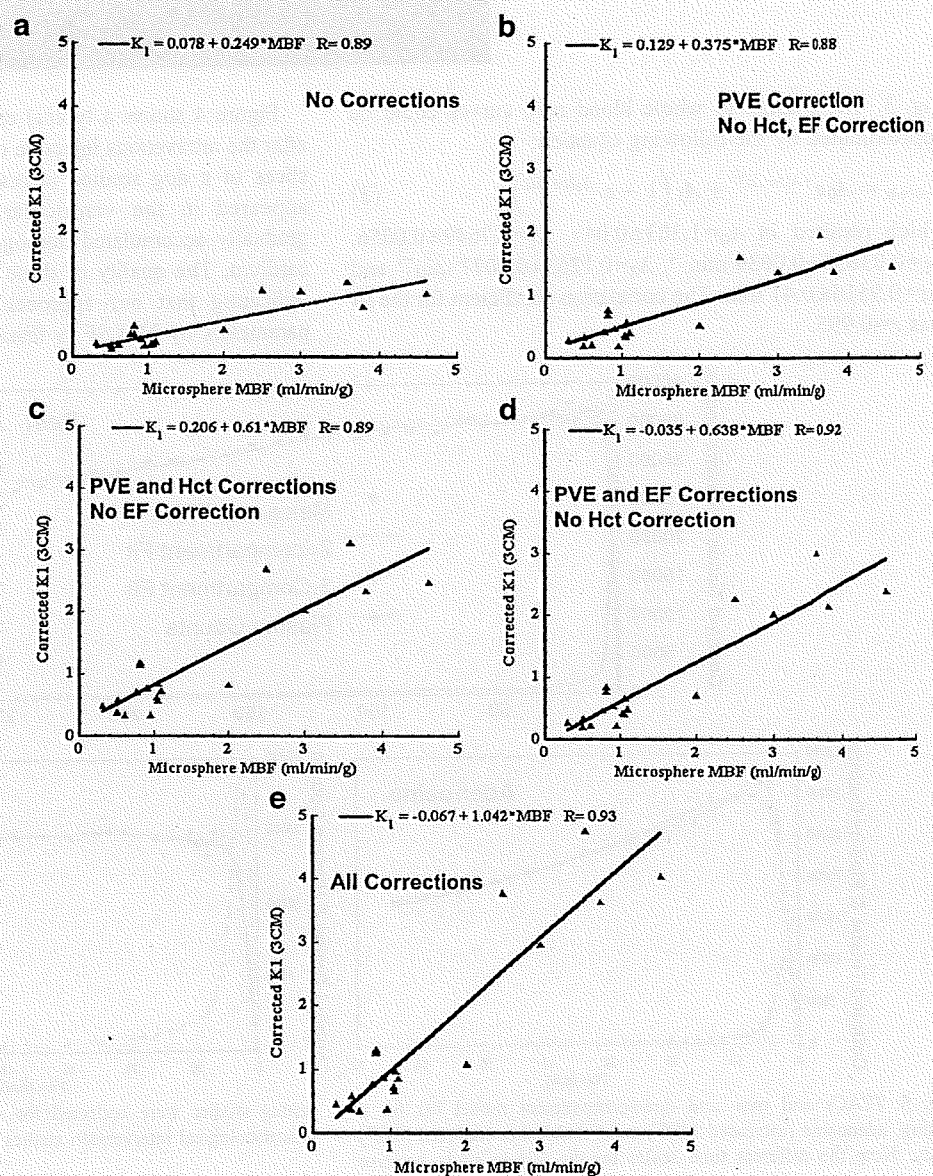


Table 1 Summary of improvement in fit with the three-compartment model over the two-compartment model

Study group	Number of curves	Mean AIC two-compartment	Mean AIC three-compartment	Mean SC two-compartment	Mean SC three-compartment	Number of curves (%) (three-compartment better than two-compartment) ^a
Resting	35	652.4	630.2 ($p < 0.01$)	663.8	638.4 ($p < 0.01$)	24 (69)
Beta-blocker	20	378.4	378.8 ($p = n.s.$)	382.0 ($p < 0.01$)	384.7	3 (15)
Adenosine	45	405.1	393.6 ($p < 0.01$)	408.7	399.5 ($p < 0.01$)	28 (62)

The p value indicates that the value in the cell is significantly lower than the corresponding other value.

AIC: Akaike information criterion, SC: Schwarz criterion

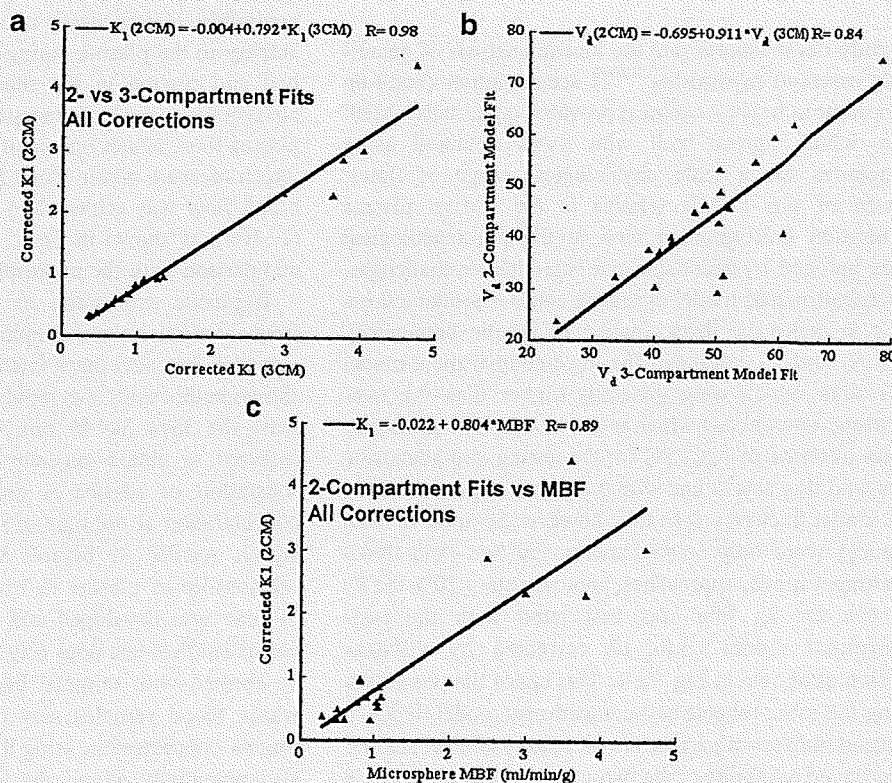
^aThis column gives the number of TTAC fits where the three-compartment model fit provided a significant improvement over the two-compartment fit according to all criteria (AIC, SC).

AIC and SC demonstrated that the three-compartment model fit provided significant improvement over the two-compartment model fit for resting and adenosine studies. For the beta-blocker studies, AIC between the two model fits was not significantly different, whilst SC demonstrated significantly better fit with the two-compartment model. Improved AIC and SC for the three-compartment model fit were observed in 69% of resting TTACs and 62% of adenosine TTACs, but only 15% in beta-blocker TTACs.

As shown in Fig. 7a and b, the K_1 and V_d values derived from the two-compartment model fit showed significant differences compared with those by the three-compartment model. Both K_1 and V_d were under-estimated with the two-compartment model fit compared with the three-compartment

model fit. It should, however, be noted that there was a good correlation between the two- and three-compartment models for K_1 , thus the bias introduced by the two-compartment model fit can potentially be corrected. K_1 values by the three-compartment model fit with all three corrections were 0.86 ± 0.36 , 2.71 ± 1.64 and 0.55 ± 0.24 ml/min/g corresponding to rest, adenosine infusion (with constant infusion at 140–700 mg/kg/h) and beta-blocker (with 2–6 mg administration), respectively. Difference in V_d was less than 10% and again this bias can potentially be corrected by the regression equation. The K_1 obtained with the two-compartment model also demonstrated a good correlation with the microsphere flow (Fig. 7c), though there was again a systematic under-estimation in K_1 .

Fig. 7 a Plot of K_1 estimates derived from the two-compartment model fit against those from the three-compartment model fit. b Plot of V_d estimates derived from the two-compartment model fit against those from the three-compartment model fit. c Plot of K_1 values derived from the two-compartment model fit against mean of the pre- and post-dynamic SPECT microsphere blood flow measurements



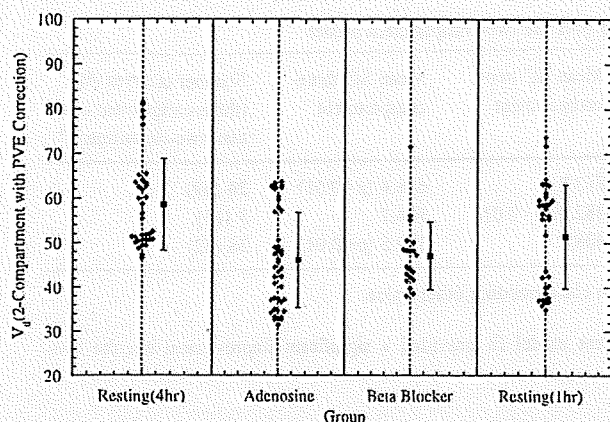


Fig. 8 V_d values obtained from the two-compartment model fit to the full 4 h resting data, adenosine and beta-blocker infusion 1 h curves and fit to first 1 h only of the resting study curves. Data from the multiple individual myocardial regions are shown

Figure 8 plots the V_d values for all evaluated myocardial segments for the fit to 4 h resting data, adenosine and beta-blocker infusion 1 h data and fit to only the first 1 h of resting data. The 4-h resting V_d values are significantly higher ($p < 0.01$) compared with the adenosine, beta-blocker values and compared with the fit to the first 1 h resting data. However, the 1-h resting values are not significantly different from the beta-blocker V_d values nor the adenosine values.

Discussion

This study demonstrates that the kinetic analysis of quantitatively assessed myocardial ^{201}Tl accumulation (build-up and washout in healthy canines) provided quantitative MBF values, which agreed well with flows obtained using microspheres for a wide physiological range of flows. The size of the TTACs relative to the arterial plasma concentration corresponded well to the pharmacological stresses induced by adenosine and beta-blocker challenges. The compartmental model approach could reproduce these TTACs to make the determination of kinetic parameters, such as K_1 and V_d , possible. The three-compartment model gave results which were generally higher than the two-compartment model and which were statistically significantly better in terms of AIC, SC for the resting and adenosine studies, and this was in line with the visual inspection of the TTAC model fit curves. It should, however, be noted that the differences were only small between the two- and three-compartment model approaches, approximately 20% for K_1 and 10% for V_d . The bias associated with the two-compartment model could be corrected by a linear regression as shown in Fig. 7a–c. This opens the possibility of using the more reliable two-compartment model fit due to its reduced number of parameters for routine clinical studies. The improved reliability of the two-compartment model fit in

the clinical setting is particularly important if one intends to shorten the study time or generate parametric images.

The three corrections for PVE, Hct and first-pass EF proved to be important. The PVE correction method used in this work cannot, however, be applied to clinical studies, and the PVE correction in the beating heart still remains a considerable challenge in clinical studies. PVE may be reduced by gating the data, which may not, however, be feasible for the already noisy and large dynamic SPECT data sets. PVE may also be reduced by including resolution recovery as part of the reconstruction process [17–20]. Alternatively, it may also be possible to include PVE as part of the kinetic model fitting [21–25]. However, this adds extra fitting parameters and requires some parameters to be assumed fixed.

The input function is an important component in compartment model fitting. In this study, rapid arterial blood sampling was performed, and the plasma was separated by centrifugation. A number of important insights were gained by performing rapid separation of plasma in a subset of samples and dogs. It was found that ^{201}Tl enters the red blood cells as observed from the rapid separation of plasma in a subset of samples and dogs, which is not un-expected as potassium is also known [22] to be taken up by the red blood cells. The exchange of ^{201}Tl between red blood cells and plasma is relatively slow compared to the passage of blood through the capillary bed and hence direct uptake of activity from the red blood cells into tissue is believed to be negligible. Hence, tissue uptake will be dominated by the activity in the plasma during passage through the capillary bed and plasma in the substrate being measured. As a consequence, the flow measurement obtained with ^{201}Tl is plasma flow, which is in contrast to the microsphere studies, which measure whole blood flow. Conversion of plasma to blood flow was achieved by dividing the plasma flow by $(1 - \text{Hct})$, as shown in Eq. 1, which then allowed the direct comparison with the microsphere measurements.

Rigorous estimation of the input function requires frequent arterial blood sampling. This is not only considered invasive, but also labor intensive. In addition, it has been shown in this study that rapid separation of the plasma for at least the first 30–40 min post- ^{201}Tl administration is required to obtain accurate plasma concentration. If the separation of plasma is delayed, then the true plasma concentration at the time of sampling cannot be measured, which results in biased K_1 estimates. An empirical relationship of plasma to whole blood ratio as a function of time was developed and was found to be sufficiently consistent between dogs (Fig. 3) to allow the mean curve to be applied with minimal bias. Thus, in clinical practice, whole blood samples may be counted and converted to plasma concentration using the empirical relationship. This also potentially allows the input function to be obtained

non-invasively from the SPECT data using, for example, a curve derived from a left ventricular region. However, it should be noted that the relationship between plasma and whole blood counts in this study was derived for a 4-min infusion protocol and may be different for other injection protocols, such as bolus injection. Previously, it has been shown that population-based input functions calibrated with one or two blood samples could avoid the need for frequent arterial blood samples [26–28]. There is also a potential for applying this approach to ^{201}Tl studies. This is beyond the scope of this study and a systematic study should be designed to confirm this in clinical settings.

^{201}Tl has a high trans-capillary EF and thus the initial regional uptake of this tracer predominantly reflects the regional blood flow [10]. Use of a tracer that has a high first-pass EF is essential when one intends to quantitatively assess MBF at a high flow range or the coronary flow reserve. The EF of ^{201}Tl is reported as >0.8 [10] for a wide flow range and is known to be higher than $^{99\text{m}}\text{Tc}$ -labelled tracers such as tetrofosmine and sestamibi [29]. The physical characteristics of ^{201}Tl are unfortunately not ideal as low energy emission increases the attenuation factor and the scatter in the image. In addition, the relatively long half-life limits the administered activity to about a tenth of that with $^{99\text{m}}\text{Tc}$ tracers. Despite these shortcomings, the physiological characteristics of having high first-pass EF make ^{201}Tl an interesting tracer particularly for the absolute quantitation of MBF and the coronary flow reserve. This study demonstrates that quantitative physiological parameters can be derived from dynamic ^{201}Tl SPECT studies, despite its less than ideal imaging characteristics.

Whilst the quantitative physiological parameter estimation removed the systematic bias between MBF estimated by ^{201}Tl dynamic SPECT and by microspheres, the spread of data points around the regression line was rather large (Figs. 6e and 7c). This is not only due to possible errors in the estimation of MBF from the ^{201}Tl , but there was also considerable variation in flow estimated by the microspheres at the beginning and end of the study. Thus, at least part of the variability is attributable to errors in microsphere flow measurement, and particularly for the pharmaceutical intervention studies, flow may not have remained constant throughout the entire study duration, which may also account for some of the differences seen between the various flow measurements.

V_d estimated in this study could serve as an index of viability, as viable myocytes are required to maintain the large concentration gradient between plasma and myocardium at equilibrium. There was no significant difference in V_d values between rest, beta-blocker and adenosine studies when fitted for 1 h (Fig. 8). The significant difference between the 1- and 4-h fit for resting data could be explained by the limitation of the two-compartment model.

Considerable spread in the V_d values observed over all dog studies on the other hand was partially attributed to the short (insufficient) scan time for reliable estimates of V_d . With the exception of the large, outlying V_d values in all 5 regions of 1 dog, the resting V_d values fell within a relatively narrow range of 47 to 65 (mean \pm SD=55 \pm 6). Given the sufficiently long scan time, significant reduction in V_d in infarcted areas may be detected. However, this would need to be tested with a suitable study design.

The scan time of 4 h required to achieve reliable V_d estimates is not practical in the routine clinical setting. As has been shown by Lau et al. [30], the scan period may be split into two sessions, an early dynamic scan for 30 min followed by a single static scan at approximately 3 h. This scheme is not more onerous than current rest/re-distribution protocols and hence could be practical. In addition, it may be possible to simplify the scanning protocol further to two static scans by using the table look-up method for the two-compartment model, which has been successfully employed for other SPECT tracers with relatively slow kinetics similar to ^{201}Tl [27, 31, 32]. This warrants further investigation.

This study relies on established, rigorous attenuation and scatter correction in SPECT [5] and availability of multi-detector SPECT systems capable of performing dynamic acquisition. To our knowledge, this is the first report that has demonstrated that it is possible to obtain quantitative physiological parameter estimates of K_1 and V_d in the myocardium using a clinical SPECT scanner and ^{201}Tl . This work suggests that it is feasible to apply our technique to clinical studies. Further studies are, however, needed to validate the proposed approach in the clinical setting. Incomplete motion correction is one possible error source, particularly in patients. Dynamic SPECT is probably more sensitive to the possible movement of patients during the study. Shortened clinical protocol is preferred, but this requires additional development to improve the reliability of parameter estimates. In addition, two scanning sessions are needed to assess the coronary flow reserve. We have recently demonstrated a technique to assess two cerebral blood flow images, one at rest and another after a vasodilating drug, from a single session of a SPECT scan in conjunction with split dose administration of ^{123}I -iodoamphetamine and dynamic SPECT [7]. As a clinical implication, the quantitative assessment of MBF and coronary flow reserve is important. For instance, coronary micro-vascular dysfunction or impaired endothelial function in patients with coronary risk factors or patients with cardiomyopathy or with heart failure is an un-resolved important issue to answer [11]. Coronary flow reserve can be reduced in patients with hypercholesterolemia without overt coronary stenosis [12]. A systematic study should be carried out to validate this approach for assessing MBF at rest and after adenosine from a single session of a scan.

Acknowledgement This study was supported by the Budget for Nuclear Research of the Ministry of Education, Culture, Sports, and Technology (MEXT), Japan; a grant from the Cooperative Link of Unique Science and Technology for Economy Revitalization promoted by the Ministry of Education, Culture, Sports and Technology, Japan and a grant for translational research from the Ministry of Health, Labour and Welfare (MHLW), Japan. We would like to thank Nihon Medi-Physics, Hyogo, Japan for providing the ^{201}Tl samples and also Mr. Yoshihide Takatani for his invaluable suggestion on the study design.

References

- Gullberg GT, Huesman RH, Ross SG, et al. Dynamic cardiac single-photon emission computed tomography. In: Beller GA, Zaret BL, editors. Nuclear cardiology: state of the art and future directions. Philadelphia, PA: Mosby-Year Book Inc.; 1998. p. 137–87.
- Chiao PC, Ficaro EP, Dayanikli F, Rogers WL, Schwaiger M. Compartmental analysis of technetium-99m-teboroxime kinetics employing fast dynamic SPECT at rest and stress. *J Nucl Med* 1994;35(8):1265–73.
- Narita Y, Eberl S, Iida H, Hutton BF, Braun M, Nakamura T, et al. Monte Carlo and experimental evaluation of accuracy and noise properties of two scatter correction methods for SPECT. *Phys Med Biol* 1996;41(11):2481–96.
- Narita Y, Iida H, Eberl S, Nakamura T. Monte Carlo evaluation of accuracy and noise properties of two scatter correction methods for ^{201}Tl cardiac SPECT. *IEEE Trans Nucl Sci* 1997;44:2465–72.
- Iida H, Shoji Y, Sugawara S, Kinoshita T, Tamura Y, Narita Y, et al. Design and experimental validation of a quantitative myocardial ^{201}Tl SPECT System. *IEEE Trans Nucl Sci* 1999;46:720–6.
- Iida H, Narita Y, Kado H, Kashikura A, Sugawara S, Shoji Y, et al. Effects of scatter and attenuation correction on quantitative assessment of regional cerebral blood flow with SPECT. *J Nucl Med* 1998;39(1):181–9.
- Kim KM, Watabe H, Hayashi T, Hayashida K, Katafuchi T, Enomoto N, et al. Quantitative mapping of basal and vasoreactive cerebral blood flow using split-dose ^{123}I -iodoamphetamine and single photon emission computed tomography. *Neuroimage* 2006;33(4):1126–35.
- Beller GA, Watson DD, Pohost GM. Kinetics of thallium distribution and redistribution: clinical applications in sequential myocardial imaging. In: Pitt B, Strauss HW, editors. Cardiovascular nuclear medicine. St. Louis: Mosby; 1979. p. 225–42.
- Berman DS, Maddhi J, Garcia EV. Role of thallium-201 imaging in the diagnosis of myocardial ischemia and infarction. In: F HS, editor. Nuclear medicine annual. New York: Raven; 1980. p. 1–55.
- Weich HF, Strauss HW, Pitt B. The extraction of thallium-201 by the myocardium. *Circulation* 1977;56(2):188–91.
- Canicci PG, Crea F. Coronary microvascular dysfunction. *N Engl J Med* 2007;356(8):830–40.
- Yokoyama I, Ohtake T, Momomura S, Nishikawa J, Sasaki Y, Omata M. Reduced coronary flow reserve in hypercholesterolemic patients without overt coronary stenosis. *Circulation* 1996;94(12):3232–8.
- Li J, Tsuji BMW, Welch A, Frey EC, Gullberg GT. Energy window optimization in simultaneous Technetium-99m and Thallium-201 SPECT data acquisition. *IEEE Trans Nucl Sci* 1995;42:1207–13.
- Meikle SR, Hutton BF, Bailey DL. A transmission-dependent method for scatter correction in SPECT. *J Nucl Med* 1994;35(2):360–7.
- Hudson HM, Larkin RS. Accelerated image reconstruction using ordered subsets of projection data. *IEEE Trans Med Imag* 1994;13:601–9.
- Choi Y, Hawkins RA, Huang SC, Brunken RC, Hoh CK, Messa C, et al. Evaluation of the effect of glucose ingestion and kinetic model configurations of FDG in the normal liver. *J Nucl Med* 1994;35(5):818–23.
- Hutton BF, Hudson HM, Beekman FJ. A clinical perspective of accelerated statistical reconstruction. *Eur J Nucl Med* 1997;24(7):797–808.
- Hutton BF, Lau YH. Application of distance-dependent resolution compensation and post-reconstruction filtering for myocardial SPECT. *Phys Med Biol* 1998;43(6):1679–93.
- Pretorius PH, King MA, Pan TS, de Vries DJ, Glick SJ, Byrne CL. Reducing the influence of the partial volume effect on SPECT activity quantitation with 3D modelling of spatial resolution in iterative reconstruction. *Phys Med Biol* 1998;43(2): 407–20.
- Soares EJ, Glick SJ, King MA. Noise characterization of combined Bellini-type attenuation correction and frequency-distance principle restoration filtering SPECT. *IEEE Trans Nucl Sci* 1996;43:3278–90.
- Iida H, Kanno I, Takahashi A, Miura S, Murakami M, Takahashi K, et al. Measurement of absolute myocardial blood flow with H_2^{15}O and dynamic positron-emission tomography. Strategy for quantification in relation to the partial-volume effect. *Circulation* 1988;78(1):104–15.
- Araujo LI, Lammertsma AA, Rhodes CG, McFalls EO, Iida H, Rechavia E, et al. Noninvasive quantification of regional myocardial blood flow in coronary artery disease with oxygen-15-labeled carbon dioxide inhalation and positron emission tomography. *Circulation* 1991;83(3):875–85.
- Bergmann SR, Herrero P, Markham J, Weinheimer CJ, Walsh MN. Noninvasive quantitation of myocardial blood flow in human subjects with oxygen-15-labeled water and positron emission tomography. *J Am Coll Cardiol* 1989;14(3):639–52.
- Iida H, Rhodes CG, de Silva R, Yamamoto Y, Araujo LI, Maseri A, et al. Myocardial tissue fraction-correction for partial volume effects and measure of tissue viability. *J Nucl Med* 1991;32(11): 2169–75.
- Iida H, Tamura Y, Kitamura K, Bloomfield PM, Eberl S, Ono Y. Histochemical correlates of (15)O-water-perfusible tissue fraction in experimental canine studies of old myocardial infarction. *J Nucl Med* 2000;41(10):1737–45.
- Iida H, Itoh H, Nakazawa M, Hatazawa J, Nishimura H, Onishi Y, et al. Quantitative mapping of regional cerebral blood flow using iodine-123-IMP and SPECT. *J Nucl Med* 1994;35(12):2019–30.
- Onishi Y, Yonekura Y, Nishizawa S, Tanaka F, Okazawa H, Ishizu K, et al. Noninvasive quantification of iodine-123-iomazenil SPECT. *J Nucl Med* 1996;37(2):374–8.
- Takikawa S, Dhawan V, Spetsieris P, Robeson W, Chaly T, Dahl R, et al. Noninvasive quantitative fluorodeoxyglucose PET studies with an estimated input function derived from a population-based arterial blood curve. *Radiology* 1993;188(1):131–6.
- Fukushima K, Momose M, Kondo C, Kusakabe K, Kasanuki H. Myocardial kinetics of (201)Thallium, (99m)Tc-tetrofosmin, and (99m)Tc-sestamibi in an acute ischemia-reperfusion model using isolated rat heart. *Ann Nucl Med* 2007;21(5):267–73.
- Lau CH, Eberl S, Feng D, Iida H, Lun PK, Siu WC, et al. Optimized acquisition time and image sampling for dynamic SPECT of Tl-201. *IEEE Trans Med Imag* 1998;17(3): 334–43.
- Iida H, Itoh H, Bloomfield PM, Munaka M, Higano S, Murakami M, et al. A method to quantitate cerebral blood flow using a rotating gamma camera and iodine-123 iodoamphetamine with one blood sampling. *Eur J Nucl Med* 1994;21(10):1072–84.
- Onishi Y, Yonekura Y, Mukai T, Nishizawa S, Tanaka F, Okazawa H, et al. Simple quantification of benzodiazepine receptor binding and ligand transport using iodine-123-iomazenil and two SPECT scans. *J Nucl Med* 1995;36(7):1201–10.

Non-invasive estimation of hepatic blood perfusion from $H_2^{15}O$ PET images using tissue-derived arterial and portal input functions

N. Kudomi · L. Slimani · M. J. Järvisalo · J. Kiss ·
R. Lautamäki · G. A. Naum · T. Savunen · J. Knuuti ·
H. Iida · P. Nuutila · P. Iozzo

Received: 30 August 2007 / Accepted: 25 March 2008 / Published online: 6 May 2008
© Springer-Verlag 2008

Abstract

Purpose The liver is perfused through the portal vein and the hepatic artery. When its perfusion is assessed using positron emission tomography (PET) and ^{15}O -labeled water ($H_2^{15}O$), calculations require a dual blood input function (DIF), i.e., arterial and portal blood activity curves. The former can be generally obtained invasively, but blood withdrawal from the portal vein is not feasible in humans. The aim of the present study was to develop a new technique to estimate quantitative liver perfusion from $H_2^{15}O$ PET images with a completely non-invasive approach.

Methods We studied normal pigs ($n=14$) in which arterial and portal blood tracer concentrations and Doppler ultrasonography flow rates were determined invasively to serve as reference measurements. Our technique consisted of using model DIF to create tissue model function and the latter method to simultaneously fit multiple liver time-activity curves from images. The parameters obtained reproduced the DIF. Simulation studies were performed to examine the magnitude of potential biases in the flow values and to optimize the extraction of multiple tissue curves from the image.

Results The simulation showed that the error associated with assumed parameters was <10%, and the optimal number of tissue curves was between 10 and 20. The estimated DIFs were well reproduced against the measured ones. In addition, the calculated liver perfusion values were not different between the methods and showed a tight correlation ($r=0.90$).

Conclusion In conclusion, our results demonstrate that DIF can be estimated directly from tissue curves obtained through $H_2^{15}O$ PET imaging. This suggests the possibility to enable completely non-invasive technique to assess liver perfusion in patho-physiological studies.

Keywords Hepatic blood flow · Input function · Portal vein · Positron emission tomography · $H_2^{15}O$

N. Kudomi (✉) · L. Slimani · M. J. Järvisalo · R. Lautamäki ·
G. A. Naum · J. Knuuti · P. Nuutila · P. Iozzo
Turku PET Centre, University of Turku,
P.O. Box 52, 20521 Turku, Finland
e-mail: nobuyuki.kudomi@tyks.fi

J. Kiss · T. Savunen
Department on Surgery, University of Turku,
Turku, Finland

H. Iida
Department of Investigative Radiology,
Advanced Medical-Engineering Center,
National Cardiovascular Center-Research Institute,
5-7-1, Fujishirodai,
Suita, Osaka 565-8565, Japan

P. Nuutila
Department of Medicine, University of Turku,
Turku, Finland

P. Iozzo
Institute of Clinical Physiology, National Research Council,
56100 Pisa, Italy

Introduction

The quantitative determination of hepatic blood flow has the potential to provide important information in the assessment and follow-up of liver disorders, which are almost invariably accompanied by abnormalities in organ